

A comparative study of nano-scale coatings on gold electrodes for bioimpedance studies of breast cancer cells

Vaishnavi Srinivasaraghavan · Jeannine Strobl · Dong Wang · James R. Heflin · Masoud Agah

Published online: 28 May 2014
© Springer Science+Business Media New York 2014

Abstract The relative sensitivity of standard gold microelectrodes for electric cell-substrate impedance sensing was compared with that of gold microelectrodes coated with gold nanoparticles, carbon nanotubes, or electroplated gold to introduce nano-scale roughness on the surface of the electrodes. For biological solutions, the electroplated gold coated electrodes had significantly higher sensitivity to changes in conductivity than electrodes with other coatings. In contrast, the carbon nanotube coated electrodes displayed the highest sensitivity to MDA-MB-231 metastatic breast cancer cells. There was also a significant shift in the peak frequency of the cancer cell bioimpedance signal based on the type of electrode coating. The results indicate that nano-scale coatings which introduce varying degrees of surface roughness can be used to

modulate the frequency dependent sensitivity of the electrodes and optimize electrode sensitivity for different bioimpedance sensing applications.

Keywords Gold nanoparticles · Carbon nanotubes · Surface roughness · Bioimpedance · ECIS · Breast cancer

1 Introduction

Bioimpedance is the complex electrical resistance of a biologically important substance. Bioimpedance measurements are increasingly being used in biomedical applications and cell research (Heileman et al. 2013; K'Owino and Sadik 2005; Spiga et al. 2014; Sun and Morgan 2010). The ease of bioimpedance measurements is a significant advantage. The technique is very rapid and requires no sample preparation, reagent costs are low, and is readily adaptable for use in high throughput devices. Bioimpedance measurements enable samples to be monitored continuously in real-time in a label-free and non-destructive fashion. Furthermore, the information content of bioimpedance is high due to the nature of the measurable electrical properties. Impedance spectroscopy is sufficiently sensitive to monitor DNA hybridization reactions; gold electrodes functionalized with a specific oligonucleotide were used to sense interactions with target DNA (Patolsky et al. 1999). Another important application of electrochemical sensing is in the measurement of medically important metabolites. Glucose monitoring has been widely studied (Heller and Feldman 2008). Similarly, serum urea and creatinine concentrations are measured using electrochemical sensors that respond to pH changes in the solution (Ho et al. 1999). Miniaturization of bioimpedance sensing platforms is simple because they require the presence of only a few electrodes and these are easily integrated with emerging microelectromechanical systems (MEMS) and microfluidic devices (Han et al. 2007; Huang et al. 2007; Pei et al. 2004).

V. Srinivasaraghavan
Bradley Department of Electrical and Computer Engineering,
Virginia Tech, 416 Whittemore Hall, 302 Whittemore (0111),
Blacksburg, VA 24061, USA
e-mail: vaishnas@vt.edu

J. Strobl
Bradley Department of Electrical and Computer Engineering,
Virginia Tech, 441 Whittemore Hall, 302 Whittemore (0111),
Blacksburg, VA 24061, USA
e-mail: jestrobl@vt.edu

M. Agah (✉)
Bradley Department of Electrical and Computer Engineering,
Virginia Tech, 469 Whittemore Hall, 302 Whittemore (0111),
Blacksburg, VA 24061, USA
e-mail: agah@vt.edu

D. Wang · J. R. Heflin
Department of Physics, Virginia Tech, Blacksburg, VA, USA

D. Wang
e-mail: wdong@vt.edu

J. R. Heflin
e-mail: rheflin@vt.edu

Electric cell-substrate impedance sensing (ECIS) is the term given to a specific type of bioimpedance measurement that is specifically applicable to measuring the impedance of adherent living cells on planar microelectrodes (Giaever and Keese 1993). ECIS has all the inherent advantages of bioimpedance measurements and a broad range of applications. In the last decade, ECIS has gained momentum as a valuable tool in cancer related studies (Abdolohad et al. 2014; Arias et al. 2010; Hong et al. 2011; Rahman et al. 2009). Researchers have demonstrated its use in monitoring cell adhesion, proliferation, motility and cytotoxicity (Wegener et al. 2000; Xiao and Luong 2003). In our laboratory, uniquely designed ECIS electrodes were used to detect rare metastatic breast cancer cells in a background of normal breast and fibroblast cells by monitoring the bioimpedance response to the histone deacetylase inhibitor suberoylanilide hydroxamic acid (Srinivasaraghavan et al. 2012). The present work is motivated by the desire to improve the sensitivity of these electrodes to detect breast cancer cells.

Here the use of nano-scale coatings as a strategy to further sensitize ECIS electrodes to bioimpedance measurements from breast cancer cells is explored. This strategy is based on two major findings. First, surface topography can be used to specifically guide the adhesion and spreading of biological cells (Lim and Donahue 2007; Stevens and George 2005). These topographies can also be tuned to control differentiation of stem cells into different lineages (Biggs et al. 2009; Christopherson et al. 2009). We predict that introducing nano-scale roughness on the surface of electrodes will help guide the cells onto the electrodes. Second, the sensitivity of neuronal recordings from implantable microelectrodes was improved using gold nanoparticle and carbon nanotube coatings (Baranauskas et al. 2011; Keefer et al. 2008; Zhang et al. 2012). In another study, glassy carbon electrodes were coated with polyaniline nanotube membranes and gold nanoparticles and the resulting electrode showed enhanced sensitivity for DNA detection (Feng et al. 2008). Coatings consisting of nanocomposites of carbon nanotubes have also been shown to improve sensitivity of electrochemical sensors (Chen et al. 2008; Hrapovic et al. 2006; Shen et al. 2008). The improved sensitivity of the electrodes in these studies was attributed to increased surface roughness and interaction or an enhanced selectivity to the target analyte. These examples provide the rationale for investigation of coatings to modulate the sensitivity of ECIS electrodes to impedance of breast cancer cells. In this work, we use coatings of gold nanoparticles (AuNP), carbon nanotubes (CNT) and electroplated gold (EPDC) to introduce nano-scale roughness on the surface of the gold electrodes and show that the sensitivity of planar gold microelectrodes can be modulated through the use of electrode coatings. To demonstrate this, first, the fabrication of these electrodes and their coating using the layer-by-layer (LbL) method and electroplating is presented. Next, the three

different nano-scale coatings along with a control (no coating), were tested with various solutions to identify the coating most sensitive to changes in conductivity. Finally, we introduced MDA-MB-231 metastatic breast cells on the same electrodes and performed a similar analysis to find the coating most sensitive to bioimpedance measurements obtained from adherent human breast cancer cells. Thus, a comparison between the control, AuNP, CNT and EPDC coatings, on the same electrode design and fabricated on the same platform is presented here and their sensitivity is investigated with respect to two specific applications, namely solution conductivity and ECIS. The results presented in this paper show promise for the use of nano-scale coated electrodes for various applications including the detection of metabolites in human fluid samples such as urine, plasma and blood and cellular drug responses.

2 Materials and methods

2.1 Fabrication

The electrode design and fabrication follow our previously published methods (Narayanan et al. 2010; Srinivasaraghavan et al. 2012) and is shown in Fig. 1(A, B). Briefly, the silicon wafers were passivated with a layer of thermal oxide (~500 nm) for electrical insulation (Fig. 1(B-a)). A positive photoresist was spun on the wafer and the electrode pattern was transferred on to it using photolithography (Fig. 1(B-b)). A thin layer of chromium/gold (Cr/Au) which is 25 nm/100 nm was deposited on the patterned wafer using e-beam evaporation (Fig. 1(B-c)). The devices were then diced and a lift-off process in acetone was used to obtain the patterned gold electrodes. For the electroplated (EPDC) electrodes, each of the patterned gold electrodes after lift-off was electroplated

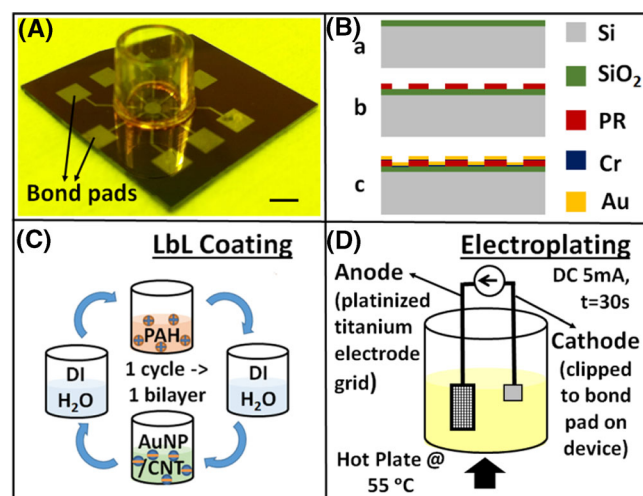


Fig. 1 **A** Photograph of the packaged bioimpedance sensor (Scale bar = 3 mm), **B** Process flow for the fabrication of the devices, **C** Process showing layer-by-layer (LbL) coating of the devices with AuNP and CNT and **D** Setup for electroplating the devices

separately in gold electroplating solution (TG-25 RTU, Technic, Inc.) heated to 55 °C, using 5 mA of direct current for 30 s. The setup for electroplating is shown in Fig. 1(D). The devices were dipped in methanol for 2 min prior to electroplating to wet the surface. The gold electroplating solution was stirred using a magnetic stir bar at 300 r/min to distribute the gold ions uniformly in solution. After electroplating, the devices were washed in methanol and deionized (DI) water and then washed again in acetone and DI water before being used for experiments.

For the gold nanoparticle (AuNP) and carbon nanotube (CNT) coatings, the devices were diced and the coatings were deposited using a layer-by-layer (LbL) method as described below. The LbL self-assembly technique was developed to fabricate dense and homogeneous thin layer coatings consisting of two materials with opposite electric charge through utilization of Coulombic attraction (Decher et al. 1992). The surface charge of a nano-scale layer of one material on the substrate will attract the second material with opposite charge. The adsorption of the second material results in reversal of the surface charge, and the steps are repeated by alternately dipping the substrate into the solutions/suspensions of these two materials. Thus, layer-by-layer coatings consisting of these two materials (two adjacent layers are called a bilayer) can be fabricated conveniently with good coating homogeneity and thickness control. The thin film coatings fabricated by the LbL technique have been applied in the electromechanical actuators (Liu et al. 2010), chemical and biological sensors (Wang et al. 2009), optical (Heflin et al. 1999) and electrochromic devices (DeLongchamp and Hammond 2004). Recently, our group used the LbL technique to selectively coat nanoparticle layers inside the micro fabricated structures of silicon for micro gas chromatography applications (Wang et al. 2013).

In this study, we used a similar approach to selectively coat gold nanoparticles (AuNP, average diameter 3.2 nm, concentration 20 ppm, Puresst Colloids Inc.) and water soluble single walled carbon nano-tubes (CNT), functionalized with *m*-polyaminobenzene sulfonic acid (PABS, Carbon Solutions Inc.) on the gold electrode via the LbL technique where the AuNP and CNT are both negatively charged. The polycation used was poly(allylamine hydrochloride) (PAH, Sigma-Aldrich), which is a long chain inert polymer and serves as an “adhesive” between every two AuNP or CNT layers holding them together. The AuNP colloid was used as received and the CNT was dissolved in de-ionized (DI) water to a concentration of 0.1 mg/ml and then was sonicated for 2 h to produce a dispersion. The pH of the CNT solution was adjusted to 8.0 (± 0.1). The PAH was made into 10 mM solution and its pH was adjusted to 4.0 (± 0.1). The process of LbL coating is summarized in Fig. 1(C). Briefly, the devices were immersed alternatively in PAH and AuNP/CNT solutions for 2.5 min each. They were also washed thrice in DI water for 30s each

time in between each coating layer. Overall, it took approximately 1 h to coat a device with 5 bilayers of AuNP or CNT.

The devices (before lift-off) were coated with AuNP (30 bilayers) or CNT (50 bilayers) using the LbL method. Then, the photoresist was removed using lift-off in acetone along with the coatings on top of it, leaving the coating only on the electrode, as shown in Fig. 2(B, C, F and G).

2.2 Experiments

The bioimpedance measurement setup has been described in detail in our previously published work (Narayanan et al. 2010). A frequency log sweep (comprising 30 points in the range 1 kHz–1 MHz) was done individually on each electrode using the impedance analyzer (Agilent HP4192A). The measured impedance magnitude ($|Z|$) and phase ($\angle Z$) values for each electrode was stored in a separate spreadsheet for each sweep.

Electrode sensitivity was measured in biological solutions of varying conductivities using DI water as the control. A phosphate buffered saline (PBS) series of concentrations 0.1X, 1X and 10X, dielectrophoresis buffer (DEP buffer) and cell culture medium were compared. DEP buffer consists of 8.5 g of sucrose and 0.725 mL of RPMI in 100 mL DI water. The cell culture medium consists of 88 mL Dulbecco's Modified Eagle Medium (DMEM): Ham's F-12 (1:1) (Lonza) with 10 mL fetal bovine serum (10 %), 1 mL penicillin-streptomycin (100 U/mL) and 1 mL L-glutamine (30 mg/mL). The conductivities of the solutions were measured using a hand-held conductivity meter. DI water had the lowest conductivity at 3.09 $\mu\text{S/cm}$. The conductivities of 0.1X, 1X and 10X PBS were 3.3, 29.4 and 209 mS/cm, respectively. DEP buffer and cell culture medium had measured conductivities of 210 and 24.7 mS/cm, respectively. Impedance measurements were made by introducing 200 μL of solution into the electrode chamber and performing a frequency sweep across all electrodes every 8 min. Impedance data were continuously recorded for 48 min to collect 6 sequential measurements on every electrode for each solution. The electrodes were washed twice using DI water between runs. The impedance of DI water was measured again after the salt solutions and between the DEP buffer and cell culture medium runs to test the reproducibility of the data and ensure that the DI water washes between measurements removed any traces of previous solutions.

Next, the MDA-MB-231 human breast cancer line (ATCC) was introduced onto the same electrodes. MDA-MB-231 cells were harvested from confluent cell cultures, suspended in growth medium (10^6 cells/mL), and 50 μL of the cell suspension (50,000 cells) were introduced into each electrode chamber; after 0.5 h to facilitate cell attachment onto the electrodes, an additional 150 μL of cell culture medium was added to maintain cell viability during experiments. Impedance

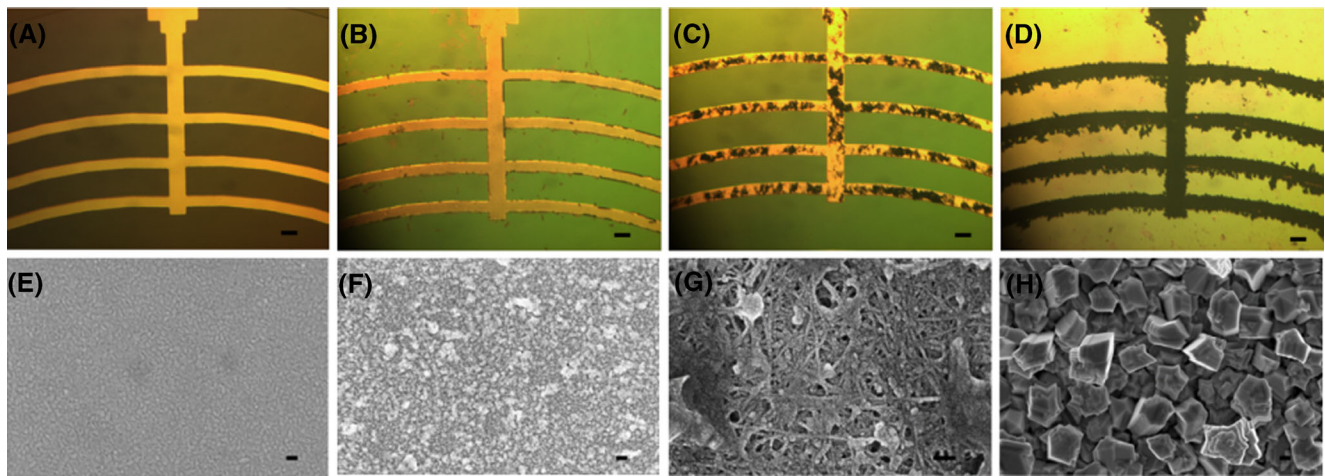


Fig. 2 Optical (A–D) and scanning electron microscope (E–H) images of the uncoated (Control—A, E), gold nanoparticle coated (AuNP—B, F), carbon nanotube coated (CNT—C, G) and DC electroplated (EPDC—D, H) electrode. Scale bar in optical images and SEM images are 50 μm and 100 nm respectively

data were recorded continuously for 24 h and yielded 180 measurements. The magnitude and phase of impedance obtained from the MDA-MB-231 cell culture at any time point ‘t’ and frequency ‘f’ is denoted by $|Z_{cell}(f,t)|$ and $\angle Z_{cell}(f,t)$, respectively. The impedance obtained from the cell culture medium at each frequency point ‘f’ was set as $Z_{no-cell}(f)$. The normalized impedance magnitude and phase at any time point ‘t’ and frequency ‘f’ are denoted by $|Z_{norm}(f,t)|$ and $\angle Z_{norm}(f,t)$ respectively and are calculated using the formulae shown in Eqs. (1) and (2).

$$|Z_{norm}(f,t)| = \frac{|Z_{cell}(f,t)| - |Z_{no-cell}(f)|}{|Z_{no-cell}(f)|} \quad (1)$$

$$\angle Z_{norm}(f,t) = \frac{\angle Z_{cell}(f,t) - \angle Z_{no-cell}(f)}{\angle Z_{no-cell}(f)} \quad (2)$$

The normalized impedance magnitude of cells over the frequency range at any time ‘t’ has a maximum value or peak value that we call the **normalized peak impedance** and occurs at a specific frequency to which we assign the name **peak frequency** ($f_{peak}(t)$). The value of normalized impedance phase corresponding to the $f_{peak}(t)$ was called the **normalized peak phase**.

2.3 Statistical tests

The statistical tests reported were performed using GraphPad Prism version 5.00 for Windows (GraphPad Software, CA, USA). Results were considered statistically significant when $P < 0.001$

3 Results and discussion

Figure 2 shows optical images of the electrodes (A–D) and scanning electron microscope (SEM) images of the surface of the nano-scale coatings on the electrodes (E–H). The control electrodes (Fig. 2(A)) are uncoated and consist only of the evaporated Cr/Au layer. The SEM image (Fig. 2(E)) shows that the surface of the control electrode is highly uniform and smooth. The AuNP, CNT and EPDC nano-scale coatings introduce varying degrees of roughness on the surface of the electrode as can be seen in Fig. 2(F, G and H). The AuNP coating (Fig. 2(F)) is relatively uniform due to the size of the gold nanoparticles used for the coating (~3.2 nm) but is not as smooth as the evaporated gold surface. The optical image of the CNT coating on the electrode shown in Fig. 2(C) shows that the coverage is non-uniform and some regions on the electrode have a thicker coating than others. This is also seen in the SEM image (Fig. 2(G)) where accumulations of CNTs are seen near the edges of the image. The SEM image shows the CNT fibers range in width between 19 and 25 nm and produce a web-like surface structure interspersed with pores whose diameters range from a few nanometers to as large as 80 nm. The EPDC coating consists of particles with jagged edges and has the largest sized particles (100–400 nm) of all the coatings that were tested in this study as is seen in the SEM image in Fig. 2(H). It is to be noted that the size of the breast cancer cells used in our experiments was about 30 μm when spread on the electrode (Srinivasaraghavan et al. 2012).

Figure 3 summarizes the impedance data obtained from cell culture medium (A), DEP buffer (B), DI water (C), PBS 0.1X (D), PBS 1X (E) and PBS 10X (F) on the control, AuNP, CNT and EPDC electrodes from 8 electrodes in 2 devices. The impedance measured in the low conductivity solutions, namely DI water and DEP buffer, was essentially identical on the control, AuNP, CNT and EPDC electrodes (Fig. 3B, C). This

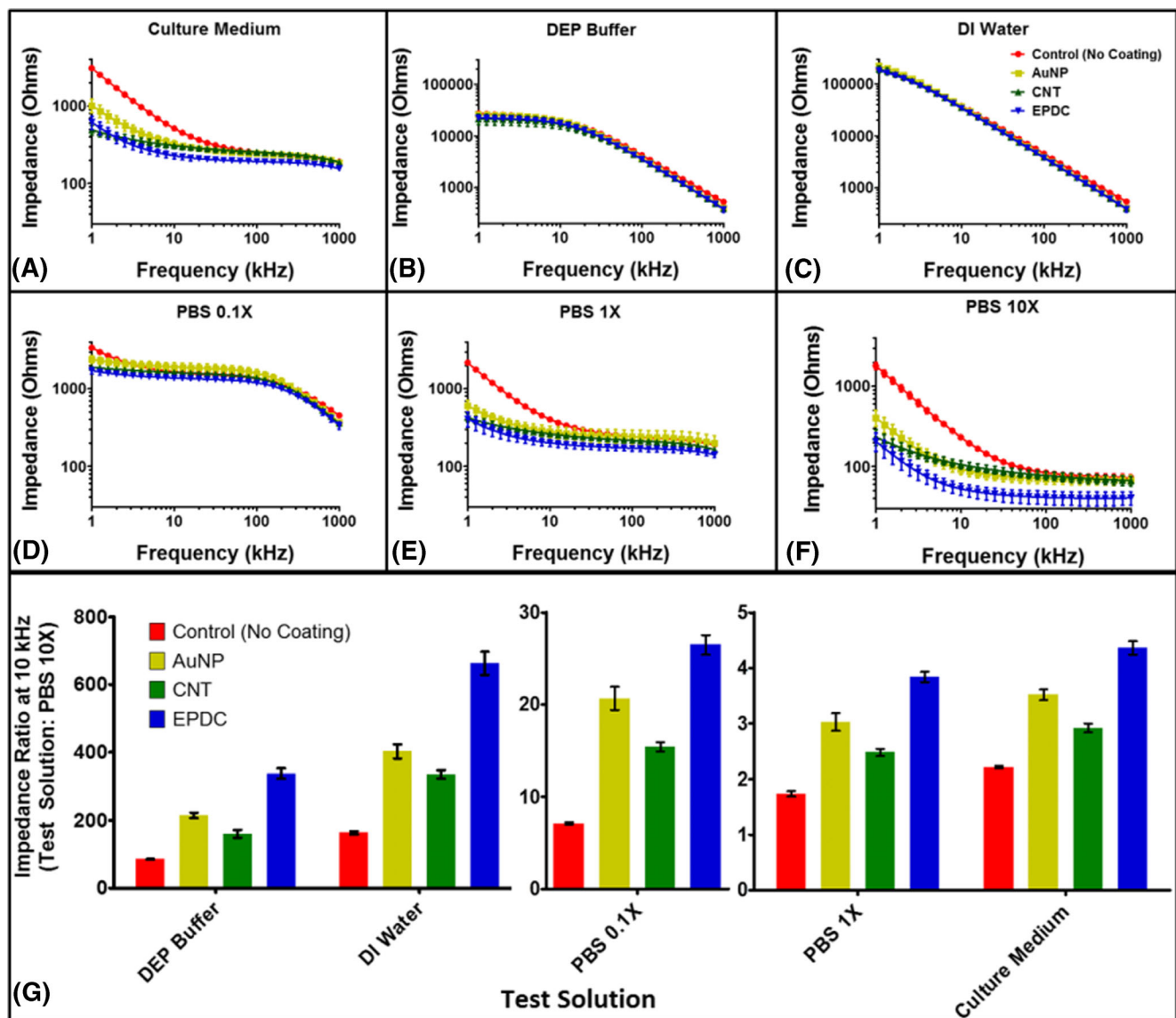


Fig. 3 A–F The impedance of solutions with varying conductivities on the electrodes with nano-scale coatings over the frequency range 1 kHz–1 MHz from $n=8$ electrodes in $N=2$ devices. Mean values are plotted and

error bars indicate SEM. **G** The ratio of impedance at 10 kHz for each solution with respect to PBS 10X on coated and uncoated electrodes

observation reflects the very low concentration of solutes. At these conductivities, the ionic reaction at the electrode-solution interface is not limited by the available surface area of the electrode, but rather, the rare interaction between solute and electrode. The frequency spectra of the impedance magnitude were distinguishable for each nano-scale electrode coating in the biological solutions with higher, more physiologically relevant conductivities. In particular, between frequencies of 1–50 kHz, the impedance magnitude tended to be greater when measured with the smoother electrode surfaces, namely, the control gold electrode and the AuNP coated electrode, than with the rougher surfaced electrodes (CNT, EPDC). This trend was observed in all the solutions with conductivities in the mS/cm range. As expected, the frequency

spectra of the impedance magnitude of the two commonly used physiological solutions, cell culture medium (24.7 mS/cm) and PBS 1X (29.4 mS/cm) were closely matched as were their conductivities.

To identify the electrode nano-scale topography providing the highest sensitivity to conductivity differences in biological solutions, the mean \pm SEM of the percent changes in the measured impedances for the cell culture medium, PBS 1X and PBS 0.1X from that of PBS 10X was computed for each electrode type. This analysis was performed across the entire bioimpedance spectra. A one-way analysis of variance (ANOVA) with a Bonferroni's multiple comparison post hoc test revealed that the percent changes in impedance in EPDC electrodes was significantly higher than other electrodes tested

($P < 0.001$). Figure 3(G) shows the ratio of impedance values at 10 kHz of all the solutions tested with respect to PBS 10X. PBS 10X was chosen because this solution had the highest conductivity as well as the lowest impedance values on all the electrode types. A comparison of the coated electrodes with the uncoated (control) electrodes reveals that the EPDC electrodes showed higher changes in impedance for the same changes in solution conductivity consistently across all solutions tested. The figure shows the comparison only at 10 kHz but this trend was observed across all frequencies tested. Thus, the EPDC electrodes were found to be most sensitive to changes in the conductivity of the test solution.

MDA-MB-231 cell suspensions in culture medium were seeded onto the same 8 electrodes in the 2 devices that were used to test the impedance of the biological solutions. Fluorescence images of the MDA-MB-231 cells stained with calcein AM (Fig. 4(A–D)) show that the cells exhibit a more stretched morphology on the control and EPDC electrodes and are more rounded with more cell-cell contacts on the AuNP and CNT electrodes. The bioimpedance spectra of the cancer cells were analyzed on each electrode, and the mean and SEM values are summarized in Fig. 4(E–G). The small variation between electrodes and devices as revealed in the SEM values plotted indicates the devices are very reliable. The nano-scale coatings on the electrodes elicit differential effects on the electrical properties of the cancer cells: normalized peak impedance magnitude (Fig. 4(E)), normalized peak phase (Fig. 4(F)) and peak frequency (Fig. 4(G)).

The initial stage of cell adhesion to the electrodes occurs during time ($t < 5$ h) and this is followed by a sustained stage of electrode attachment ($t \geq 5$ h–24 h). During the initial stage, values of all three measured electrical parameters showed

some random variability. During the sustained stage, several electrode-specific patterns of emerged.

The magnitude of the normalized peak impedance (Fig. 4(E)) is a well-accepted index of the nature of the cell-electrode interaction. Based on the magnitude of the bioimpedance, there is initially a somewhat stronger level of cancer cell adhesion to the AuNP nano-coated electrodes compared with the other electrode surfaces. However, electrical measurements from the AuNP-coated electrodes displayed certain anomalies during the sustained stage making AuNP-coated electrodes impractical for monitoring sustained electrical properties in the cancer cells. The underlying cause for these shifts is not certain, however, AuNP are readily taken up by cancer cells, raising the possibility that physical interactions between the cancer cells and the 3.2 nm AuNP are involved (Trono et al. 2011).

In contrast, cell adhesion is initially weaker to the other three electrode types compared to the AuNP-coated electrodes, but cell adhesion gradually strengthens during the entire sustained stage as monitored by the rise in bioimpedance magnitude (Fig. 4(E)). This is particularly evident in the case of the CNT nanostructures. Structural similarities between the nano-scale web-like patterns created by the CNT on the gold electrodes and the electrospun collagen networks produced as simulated extracellular matrix for tissue engineering might foster the strong adhesion to the CNT-modified gold electrodes (Lin et al. 2013). We observed that the CNT electrodes have the maximum normalized values for both peak impedance and peak phase. A one-way ANOVA with Bonferroni's multiple comparison post hoc test confirmed that the CNT electrodes showed significantly higher changes in both peak normalized impedance ($P < 0.001$) and

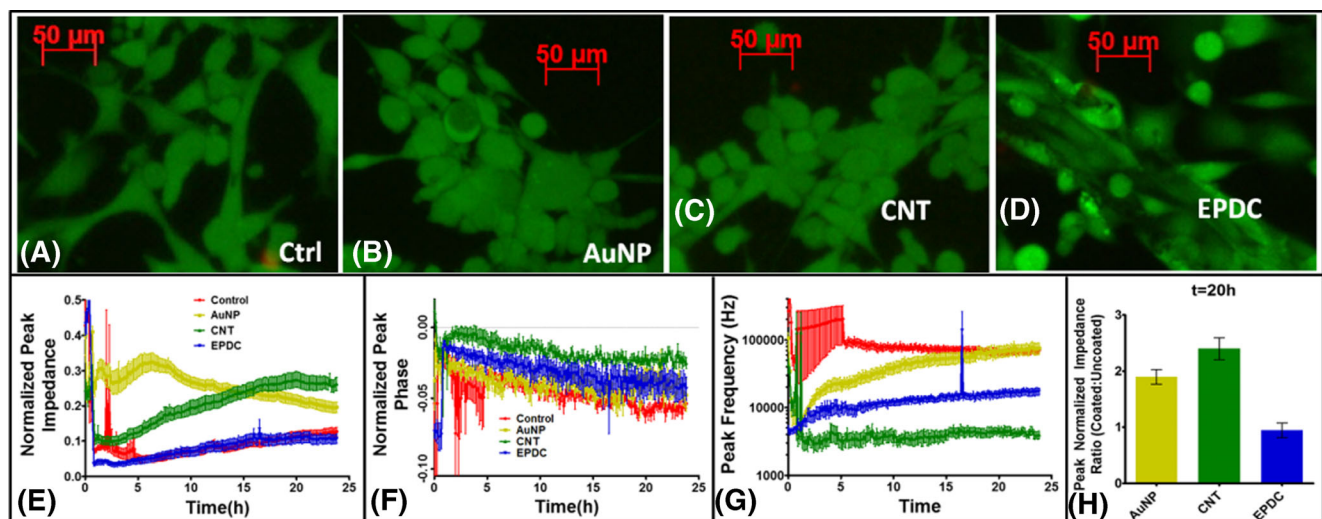


Fig. 4 A–D Fluorescence images of the MDA-MB-231 cells on the electrodes. Normalized peak magnitude **E**, normalized peak phase **F** and peak frequency **G** of the impedance of MDA-MB-231 cells on the control, AuNP, CNT and EPDC electrodes in 24 h after cell seeding. **H**

The ratio of normalized peak impedance magnitude at $t = 20$ h of AuNP, CNT and EPDC coated electrodes with respect to the uncoated (control) electrodes. Data shown is from $n = 8$ electrodes in $N = 2$ devices. Mean values are plotted and error bars indicate SEM

peak normalized phase ($P < 0.001$) in the presence of MDA-MB-231 cells. Figure 4(H) shows the ratio of the normalized peak impedance magnitude at $t = 20$ h on the AuNP, CNT and EPDC electrodes with respect to the uncoated control electrodes. The figure clearly shows that the impedance change in response to metastatic breast cancer cells is maximal on the CNT coated electrodes followed by the AuNP electrodes. Also, the EPDC electrode response is not significantly different from that of the control electrodes in the presence of breast cancer cells.

The most interesting finding of this study was the distribution of the average peak frequency ($t > 10$ h) of the MDA-MB-231 cells on the control (79.7 ± 7.4 kHz), CNT (3.8 ± 0.9 kHz) and EPDC (20.1 ± 3.9 kHz) electrodes over the frequency spectrum (Fig. 4(G)). It should also be noted that the peak frequency values for each electrode coating are stable after $t = 10$ h with less than 25 % variation thereafter. The shift in peak frequency from control gold electrodes was significant on both electrode coatings and was greatest on the CNT electrodes. The fluorescence images in Fig. 4(A, C, D) show cell morphology changes occur in response to these coatings, and this might be a factor in the bioimpedance frequency shift. This is the first demonstration that electrode coatings can be used to modulate the peak bioimpedance frequency of a cell, and opens a new avenue of research in engineering nanocomposite electrode coatings as a means to detect different types of cells based upon their impedance spectra. Further research will be directed towards investigation of the sensitivity of these coated electrodes to normal and other types of cancerous breast cells as well as the exploration of additional nanocomposite coatings.

4 Conclusion

Thus, planar gold microelectrodes were successfully coated with AuNP and CNT using a layer-by-layer deposition method as well as electroplated gold to create nano-scale roughness on the surface of the electrodes. The nano-scale coatings resulted in improved sensitivity of these electrodes but the type of coating that was most sensitive differed for the two applications tested. Experiments on the impedance of biologically relevant solutions with varying conductivities revealed that the EPDC electrodes displayed the highest sensitivity to changes in conductivity. The changes in the impedance due to the adherence of metastatic breast cells were most significant on the CNT-coated electrodes. We showed that nano-scale coatings can shift the frequency dependent sensitivity of the electrodes and suggest that such coatings might therefore be applied to resolution of the bioimpedance spectra of cancer from non-cancerous cells. Further studies on coatings with ordered nano-scale features could further enhance the sensitivity to the cells.

Acknowledgments We would like to thank Mr. Stephen McCartney from the Nanoscale Characterization and Fabrication Laboratory (NCFL) at the Institute for Critical Technology and Applied Science (ICTAS) for his guidance in obtaining the scanning electron microscope images shown here. We would also like to thank Mr. Hamza Shakeel for his support with electroplating the devices. This work was supported by the National Science Foundation under ECCS award number 0925945.

References

- M. Abdolhad, H. Shashaani, M. Janmaleki, S. Mohajerzadeh, Silicon nanoglass based impedance biosensor for label free detection of rare metastatic cells among primary cancerous colon cells, suitable for more accurate cancer staging. *Biosens. Bioelectron.* **59**, 151–159 (2014)
- L.R. Arias, C.A. Perry, L.J. Yang, Real-time electrical impedance detection of cellular activities of oral cancer cells. *Biosens. Bioelectron.* **25**(10), 2225–2231 (2010)
- G. Baranauskas, E. Maggiolini, E. Castagnola, A. Ansaldo, A. Mazzoni, G.N. Angotzi, A. Vato, D. Ricci, S. Panzeri, L. Fadiga, Carbon nanotube composite coating of neural microelectrodes preferentially improves the multiunit signal-to-noise ratio. *J. Neural Eng.* **8**(6), 12 (2011)
- M.J.P. Biggs, R.G. Richards, N. Gadegaard, R.J. McMurray, S. Affrossman, C.D.W. Wilkinson, R.O.C. Oreffo, M.J. Dalby, Interactions with nanoscale topography: adhesion quantification and signal transduction in cells of osteogenic and multipotent lineage. *J. Biomed. Mater. Res. Part A* **91A**(1), 195–208 (2009)
- J. Chen, W.-D. Zhang, J.-S. Ye, Nonenzymatic electrochemical glucose sensor based on MnO₂/MWNTs nanocomposite. *Electrochem. Commun.* **10**(9), 1268–1271 (2008)
- G.T. Christopherson, H. Song, H.Q. Mao, The influence of fiber diameter of electrospun substrates on neural stem cell differentiation and proliferation. *Biomaterials* **30**(4), 556–564 (2009)
- G. Decher, J.D. Hong, J. Schmitt, Buildup of ultrathin multilayer films by a self-assembly process. 3. Consecutively alternating adsorption of anionic and cationic polyelectrolytes on charged surfaces. *Thin Solid Films* **210**(1–2), 831–835 (1992)
- D.M. DeLongchamp, P.T. Hammond, Multiple-color electrochromism from layer-by-layer-assembled polyaniline/Prussian Blue nanocomposite thin films. *Chem. Mater.* **16**(23), 4799–4805 (2004)
- Y.Y. Feng, T. Yang, W. Zhang, C. Jiang, K. Jiao, Enhanced sensitivity for deoxyribonucleic acid electrochemical impedance sensor: Gold nanoparticle/polyaniline nanotube membranes. *Anal. Chim. Acta.* **616**(2), 144–151 (2008)
- I. Giaever, C.R. Keese, A morphological biosensor for mammalian-cells. *Nature* **366**(6455), 591–592 (1993)
- A. Han, L. Yang, A.B. Frazier, Quantification of the heterogeneity in breast cancer cell lines using whole-cell impedance spectroscopy. *Clin. Cancer Res.* **13**(1), 139–143 (2007)
- J.R. Hefflin, C. Figura, D. Marciu, Y. Liu, R.O. Claus, Thickness dependence of second-harmonic generation in thin films fabricated from ionically self-assembled monolayers. *Appl. Phys. Lett.* **74**(4), 495–497 (1999)
- K. Heileman, J. Daoud, M. Tabrizian, Dielectric spectroscopy as a viable biosensing tool for cell and tissue characterization and analysis. *Biosens. Bioelectron.* **49**, 348–359 (2013)
- A. Heller, B. Feldman, Electrochemical glucose sensors and their applications in diabetes management. *Chem. Rev.* **108**(7), 2482–2505 (2008)
- W.O. Ho, S. Krause, C.J. McNeil, J.A. Pritchard, R.D. Armstrong, D. Athey, K. Rawson, Electrochemical sensor for measurement of urea and creatinine in serum based on ac impedance measurement of

- enzyme-catalyzed polymer transformation. *Anal. Chem.* **71**(10), 1940–1946 (1999)
- J. Hong, K. Kandasamy, M. Marimuthu, C.S. Choi, S. Kim, Electrical cell-substrate impedance sensing as a non-invasive tool for cancer cell study. *Analyst* **136**(2), 237–245 (2011)
- S. Hrapovic, E. Majid, Y. Liu, K. Male, J.H.T. Luong, Metallic nanoparticle-carbon nanotube composites for electrochemical determination of explosive nitroaromatic compounds. *Anal. Chem.* **78**(15), 5504–5512 (2006)
- C.-J. Huang, Y.-H. Chen, C.-H. Wang, T.-C. Chou, G.-B. Lee, Integrated microfluidic systems for automatic glucose sensing and insulin injection. *Sens. Actuators B-Chem.* **122**(2), 461–468 (2007)
- I.O. K' Owino, O.A. Sadik, Impedance spectroscopy: a powerful tool for rapid biomolecular screening and cell culture monitoring. *Electroanalysis* **17**(23), 2101–2113 (2005)
- E.W. Keefer, B.R. Botterman, M.I. Romero, A.F. Rossi, G.W. Gross, Carbon nanotube coating improves neuronal recordings. *Nat. Nanotechnol.* **3**(7), 434–439 (2008)
- J.Y. Lim, H.J. Donahue, Cell sensing and response to micro- and nanostructured surfaces produced by chemical and topographic patterning. *Tissue Eng.* **13**(8), 1879–1891 (2007)
- H.Y. Lin, Y.J. Kuo, S.H. Chang, T.S. Ni, Characterization of electrospun nanofiber matrices made of collagen blends as potential skin substitutes. *Biomed. Mater.* **8**(2), 9 (2013)
- S. Liu, R. Montazami, Y. Liu, V. Jain, M.R. Lin, X. Zhou, J.R. Heflin, Q.M. Zhang, Influence of the conductor network composites on the electromechanical performance of ionic polymer conductor network composite actuators. *Sens. Actuators a-Phys.* **157**(2), 267–275 (2010)
- S. Narayanan, M. Nikkhah, J.S. Strobl, M. Agah, Analysis of the passivation layer by testing and modeling a cell impedance micro-sensor. *Sens. Actuators a-Phys.* **159**(2), 241–247 (2010)
- F. Patolsky, E. Katz, A. Bardea, I. Willner, Enzyme-linked amplified electrochemical sensing of oligonucleotide-DNA interactions by means of the precipitation of an insoluble product and using impedance spectroscopy. *Langmuir* **15**(11), 3703–3706 (1999)
- J.H. Pei, F. Tian, T. Thundat, Glucose biosensor based on the microcantilever. *Anal. Chem.* **76**(2), 292–297 (2004)
- A.R.A. Rahman, C.M. Lo, S. Bhansali, A detailed model for high-frequency impedance characterization of ovarian cancer epithelial cell layer using ECIS electrodes. *IEEE Trans. Biomed. Eng.* **56**(2), 485–492 (2009)
- Q. Shen, S.K. You, S.G. Park, H. Jiang, D.D. Guo, B.A. Chen, X.M. Wang, Electrochemical Biosensing for cancer cells based on TiO₂/CNT nanocomposites modified electrodes. *Electroanalysis* **20**(23), 2526–2530 (2008)
- F.M. Spiga, A. Bonyar, B. Ring, M. Onofri, A. Vinelli, H. Santha, C. Guiducci, G. Zuccheri, Hybridization chain reaction performed on a metal surface as a means of signal amplification in SPR and electrochemical biosensors. *Biosens. Bioelectron.* **54**, 102–108 (2014)
- V. Srinivasaraghavan, J. Strobl, M. Agah, Bioimpedance rise in response to histone deacetylase inhibitor is a marker of mammary cancer cells within a mixed culture of normal breast cells. *Lab Chip* **12**(24), 5168–5179 (2012)
- M.M. Stevens, J.H. George, Exploring and engineering the cell surface interface. *Science* **310**(5751), 1135–1138 (2005)
- T. Sun, H. Morgan, Single-cell microfluidic impedance cytometry: a review. *Microfluid. Nanofluid.* **8**(4), 423–443 (2010)
- J.D. Trono, K. Mizuno, N. Yusa, T. Matsukawa, K. Yokoyama, M. Uesaka, Size, concentration and incubation time dependence of gold nanoparticle uptake into pancreas cancer cells and its future application to x-ray drug delivery system. *J. Radiat. Res.* **52**(1), 103–109 (2011)
- D. Wang, H. Shakeel, J. Lovette, G.W. Rice, J.R. Heflin, M. Agah, Highly stable surface functionalization of Microgas chromatography columns using layer-by-layer self-assembly of silica nanoparticles. *Anal. Chem.* **85**, 8135–8141 (2013)
- Z.Y. Wang, J.R. Heflin, K. Van Cott, R.H. Stolen, S. Ramachandran, S. Ghalmi, Biosensors employing ionic self-assembled multilayers adsorbed on long-period fiber gratings. *Sens. Actuators B-Chem.* **139**(2), 618–623 (2009)
- J. Wegener, C.R. Keese, I. Giaever, Electric cell-substrate impedance sensing (ECIS) as a noninvasive means to monitor the kinetics of cell spreading to artificial surfaces. *Exp. Cell Res.* **259**(1), 158–166 (2000)
- C. Xiao, J.H.T. Luong, On-line monitoring of cell growth and cytotoxicity using electric cell-substrate impedance sensing (ECIS). *Biotechnol. Prog.* **19**(3), 1000–1005 (2003)
- H.N. Zhang, J. Shih, J. Zhu, N.A. Kotov, Layered nanocomposites from gold nanoparticles for neural prosthetic devices. *Nano Lett.* **12**(7), 3391–3398 (2012)